J. Membrane Biol. 211, 15–25 (2006)
DOI: 10.1007/s00232-005-7008-6

The Journal of
Membrane
Biology

Use of Steady-State Laurdan Fluorescence to Detect Changes in Liquid Ordered Phases in Human Erythrocyte Membranes

Rebekah Vest, Rachel Wallis, Lauren B. Jensen, Andrea C. Haws, Joseph Callister, Brent Brimhall, Allan M. Judd, John D. Bell
Department of Physiology and Developmental Biology, Brigham Young University, Provo, Utah 84602

Received: 28 September 2005/Accepted: 22 March 2006

Abstract. In artificial phospholipid bilayers, dual measurements of laurdan steady-state anisotropy and emission spectra can be used to identify the presence of liquid ordered phases. Human erythrocytes were used as a model to test whether similar measurements could be applied to biological samples. Specifically, laurdan anisotropy and emission spectra were obtained from native erythrocytes before and after treatment with calcium ionophore and from the microvesicles (known to be enriched in liquid ordered domains) shed from the cells during calcium entry. Spectral and anisotropy data were consistent with an increased order and reduced fluidity of erythrocyte membrane lipids upon ionophore treatment. Microvesicle membranes appeared more ordered than native erythrocytes and similar to ionophore-treated cells based on laurdan emission. In contrast, the anisotropy value was lower in microvesicles compared to ionophore-treated cells, suggesting greater probe mobility. Parallel measurements of diphenylhexatriene anisotropy corroborated the laurdan data. These results were consistent with the liquid ordered property of microvesicle membranes based on comparisons to behavior in artificial membranes. Two-photon microscopy was used to examine the distribution of laurdan fluorescence along the surface of erythrocyte membranes before and after ionophore treatment. A dual spatial analysis of laurdan anisotropy, as revealed by the distribution of laurdan emission spectra, and intensity excited by polarized light suggested that the plasma membranes of ionophore-treated erythrocytes may also exhibit elevated numbers of liquid ordered domains.

Key words: Erythrocyte vesiculation — Phospholipase A_2 — Raft — Generalized polarization — Anisotropy — Biophysical technique — Fluorescent probe

Correspondence to: John D. Bell; email: john_bell@byu.edu

Introduction

Recently, there has been growing interest in membrane structures known as lipid rafts. *Rafts* are detergent-resistant membrane domains consisting primarily of cholesterol and sphingomyelin and enriched in glycosylphosphatidylinositol (Barenholz, 2004; Brown, 2002; Simons & Ikonen, 1997; Simons & Toomre, 2000). Furthermore, a broad range of evidence from both model and biological membranes indicates that the lipids in rafts display the physical properties of a liquid ordered phase (Barenholz, 2004; Brown, 2002; Ge et al., 1999).

Although several methods for visualizing or detecting the presence of liquid ordered domains in biological membranes have been described (Bacia et al., 2004; Gaus et al., 2003; Gidwani et al., 2001; Kindzelskii et al., 2004; Scheiffele et al., 1999), attempts have not been made to explore changes in the prevalence of such domains in real time during acute experimental treatments. Nevertheless, recent work has suggested that the fluorescent probe laurdan may serve as a useful probe for detecting such changes in membrane structure (Harris et al., 2002). The shape of its emission spectrum readily distinguishes solid ordered and liquid disordered phases due to a large sensitivity of the probe to solvent polarity (Parasassi et al., 1991). Moreover, when the data from these spectral measurements are combined with assessments of laurdan anisotropy, the liquid ordered phase can be distinguished from other phases. This distinction is possible because the laurdan spectrum is more sensitive to lipid order than membrane fluidity, whereas anisotropy is sensitive to both (Harris et al., 2002).

Since laurdan emission spectra and anisotropy can be obtained simultaneously from a membrane sample in real time, we explored whether laurdan could be a useful tool for detecting and studying changes in liquid ordered prevalence during experimental perturbation. We examined this possibility using human erythrocytes as a simple model of biological membranes in which the amount of liquid ordered structure could be manipulated. This manipulation involves using a calcium ionophore to stimulate the shedding of microvesicles from the cell membrane (Allan et al., 1980; Chukhlovin, 1996; Fourcade et al., 1995; Salzer et al., 2002; Smith et al., 2001).

Microvesicles are about 60–200 nm in diameter and display a number of characteristics that distinguish their membranes from those of intact erythrocytes (Allan et al., 1980; Salzer et al., 2002). Most important for this study, they possess an increased prevalence of liquid ordered lipid compared to the parent membrane (Salzer et al., 2002). Moreover, they are enriched in glycosylphosphatidylinositol-linked proteins (due to the prevalence of lipid rafts), lack certain cytoskeletal elements, lack the normal asymmetrical distribution of phospholipid species across the bilayer, and are susceptible to the hydrolytic action of secretory phospholipase A_2 ($sPLA_2$) (Butikofer et al., 1989; Comfurius et al., 1990; Fourcade et al., 1995; Salzer et al., 2002).

Accordingly, laurdan emission spectra and anisotropy data were gathered from human erythrocytes before and after ionophore treatment. Results obtained from the original cells were compared to those identified for microvesicles shed from those cells. 1,6-Diphenyl-1,3,5-hexatriene (DPH), a probe that has been used commonly to study membrane dynamics, is included for comparison. The results demonstrate that laurdan can detect changes in the prevalence of liquid ordered domains in biological membranes.

Materials and Methods

Materials

Acrylodan-derivatized fatty acid binding protein (ADIFAB), DPH, and 6-dodecanoyl-2-dimethylaminonaphthalene (laurdan) were purchased from Molecular Probes (Eugene, OR). Factor Va, factor Xa, and prothrombin were obtained from Hematologic Technologies (Essex Junction, VT). Thrombin substrate was acquired from Calbiochem (La Jolla, CA). Dipalmitoylphosphatidylcholine (DPPC) was purchased from Avanti Polar Lipids (Birmingham, AL). Cholesterol was from Spectrum (Gardena, CA). $sPLA_2$ was isolated from the venom of *Agkistrodon piscivorus piscivorus* according to published procedures (Maraganore et al., 1984). The protein was stored as a lyophilized powder at −20°C. Stock solutions of the enzyme were suspended at a concentration of 100 μg/ml in 50 mM KCl (including 3 mM NaN_3 as a preservative) and stored at 4°C. Multilamellar vesicles composed of either 100% DPPC or 70% DPPC with 30% cholesterol were prepared and suspended in 20 mM sodium citrate buffer (pH 7.0) with 150 mM KCl as described (Harris et al., 2002).

Microvesicle Isolation

Human erythrocytes were obtained from blood samples remaining after physical exams at the Brigham Young University Student Health Center. Samples were collected in ethylenediaminetetraacetic acid (EDTA) vacutainers and stored overnight at 4°C. Erythrocytes were centrifuged and the plasma layer and buffy coat removed. MBSS (134 mM NaCl, 6.2 mM KCl, 1.6 mM $CaCl_2$, 1.2 mM $MgCl_2$, 18.0 mM 4-[2-hydroxyethyl]-1-piperazineethanesulfonic acid [HEPES], and 13.6 mM glucose, pH 7.4, 37°C) was added to restore the sample to the original hematocrit. Washed erythrocytes (3 ml) were combined with 24 ml MBSS plus ionomycin (2.8 μM) and incubated for 1 h at 37°C with occasional gentle mixing. After incubation, the erythrocytes were removed by centrifugation in a swinging bucket rotor (4°C, $600 \times g$, 15 min). An aliquot of the supernatant was then examined under a microscope to verify the absence of erythrocytes. If cells were present, the centrifugation step was repeated. Microvesicles were then concentrated by centrifugation at higher velocity (4°C, $22{,}000 \times g$, 40 min). The majority of the supernatant was discarded, and the pellet was dispersed in the remaining liquid (approximately 1 ml) to yield a more concentrated suspension and stored at 4°C. The protein concentration of each preparation was quantified using the method of Bradford (1976). The characterizations of the vesicles described in the sections below were completed within 1 week of preparation and conducted in a different sequence in each case to avoid possible systematic errors associated with vesicle age.

Fluorescence Spectroscopy

Steady-state fluorescence was monitored using photon-counting spectrofluorometers (Fluoromax from Jobin Yvon, Edison, NJ; or PC1 from ISS, Champaign, IL). For laurdan experiments on liposomes or isolated microvesicles, samples (50 μM lipid in the case of liposomes and about 25 μg/ml protein in the case of microvesicles) were incubated in 2 ml citrate/KCl buffer (liposomes) or MBSS (microvesicles) containing 2.5 μM laurdan (in dimethyl sulfoxide, DMSO) until fluorescence was stable, and fluorescence intensity was assessed at 435 and 500 nm (excitation = 350 nm) at 37°C. Generalized polarization (GP) values were calculated from the intensities after they reached steady state as described (Parasassi et al., 1991). Experiments were repeated with erythrocytes (0.075% hematocrit (hct) in MBSS) instead of microvesicles to obtain control values. Background stray or scattered light (microvesicles or erythrocytes without fluorophore) was negligible.

In some cases, erythrocytes (0.075% hct) were incubated with laurdan or DPH in the fluorometer as described above and both emission spectra (laurdan) and anisotropy (laurdan and DPH, see details below) values were then acquired. Ionomycin (300 nM) was then added to the sample, and spectra and anisotropy measurements were repeated following 10 min incubation. Cells were removed by centrifugation ($3{,}300 \times g$, 5 min) and the measurements repeated. Residual fluorescence not associated with microvesicles was quantified by removing the microvesicles via centrifugation ($13{,}200 \times g$, 15 min) and assessing the fluorescence intensity remaining in the supernatant. This lingering fluorescence was generally negligible, indicating that the majority of measured fluorescence was associated with cells and microvesicles.

Anisotropy measurements were obtained with the PC1 fluorometer in the L-format equipped with Glan-Thompson polarizers and 16 nm bandpass on both monochromators. Samples were prepared as described above for steady-state emission intensity.

Fluorescence intensity at 435 nm (laurdan) or 452 nm (DPH) and excited at 350 nm was measured with excitation and emission polarizers parallel to each other (both at 0°, I_0) and repeated with the polarizers perpendicular (excitation 0°, emission 90°, I_{90}). The intensity of scattered light was measured at each permutation of polarizer angles using erythrocytes without fluorescent probe under the various treatment conditions described in the previous paragraph and subtracted from the relevant data prior to calculating the anisotropy. Effects of sample turbidity on anisotropy were excluded by diluting samples and demonstrating a lack of effect on anisotropy values. An analogous process was used to obtain anisotropy values for liposomes (50 μM lipid). Anisotropy was calculated using the traditional equation:

$$r = \frac{I_0 - GI_{90}}{I_0 + 2GI_{90}} \quad (1)$$

The correction factor (G) was obtained from the ratio of emission intensity at 0° and 90° with the excitation polarizer oriented at 90°.

An important concern when interpreting steady-state anisotropy values under different experimental conditions is whether the excited state lifetime of the probe differs among those conditions. This concern is relevant to laurdan since changes in GP values correspond to altered lifetimes due to the solvent relaxation phenomenon. This obstacle can be overcome by obtaining time-resolved anisotropy data or by measuring probe lifetimes under the various experimental conditions and analyzing the data accordingly, as addressed previously (Harris et al., 2002). We applied the same analysis to the anisotropy data obtained in this study. The differences in anisotropy upon addition of ionomycin to cells were not due to lifetime artifacts since the increased GP values in treated cells would correspond to increased lifetime and therefore a decrement in the observed anisotropy rather than the increment that was observed. Consequently, the changes in anisotropy are probably conservative and the actual differences may be slightly larger than those shown (see below). The data comparing microvesicles to treated cells were not subject to lifetime artifacts since the value of anisotropy changed when GP remained constant. The two-photon data were potentially complicated by changes in laurdan lifetime since GP and anisotropy changed in opposite directions. Application of the calculations described in Harris et al. (2002) revealed that only a 4–8% reduction in anisotropy would be expected given the magnitude of the difference in GP between control and treated cells. This potential artifact was much smaller than the corresponding change in the apparent anisotropy shown below.

Phosphatidylserine Exposure

Phosphatidylserine (PS) exposure was assayed based on prothrombinase activity using a variation of the method of de Jong and Ott (1993). Preparations of erythrocytes for controls were diluted to about 6% hct. Two preparations of each sample were made: one suspended in normal MBSS and the other in hypotonic MBSS (MBSS diluted to 10% in distilled water). The sample suspended in 10% MBSS was frozen in liquid nitrogen, removed, and thawed immediately prior to use. This lysed sample provided a standard for 100% PS exposure for erythrocytes. Microvesicle samples were treated similarly but without dilution in hypotonic buffer (the freeze/thaw cycle was sufficient to fully expose PS in aliquots of microvesicle samples). Factor Va (6 nM final), factor Xa (3 nM final) and 1 μl erythrocyte or microvesicles were added to 25 μl of buffer containing 10 nM Tris-HCl, 136 mM NaCl, 2.7 mM KCl, 4 mM $CaCl_2$, and 0.5 mg/ml bovine serum albumin at pH 7.9. The mixture was incubated at 37°C for 2 min before adding prothrombin (4 μM final, dissolved in a solution of 5.6 mM $CaCl_2$ and 0.5 mg/ml bovine serum albumin). The activation reaction (in 30 μl final volume) was then allowed to continue for 5 min, at which time it was quenched by adding the mixture to 920 μl of prewarmed buffer (50 mM Tris-HCl, 120 mM NaCl, 2 mM EDTA, pH 7.5) in a spectrophotometer sample cell. The spectrophotometer absorbance was adjusted to 0, 50 μl of thrombin substrate II (100 μM final) was added, and absorbance (at 405 nm) was recorded for 6 min. The percentage of PS exposure was determined by dividing each sample absorbance by the absorbance of the corresponding lysed standards.

Susceptibility to $sPLA_2$

Susceptibility of erythrocytes and microvesicles to $sPLA_2$ was monitored using the fluorescent fatty acid binding protein ADIFAB (Richieri and Kleinfeld, 1995). Washed erythrocytes (0.075% hct) or microvesicle samples (about 25 μg/ml protein) were prepared for fluorescence spectroscopy as described above. Fluorescence emission was monitored over time at dual wavelengths (excitation = 390 nm, emission 432 and 505 nM) (Richieri and Kleinfeld, 1995). ADIFAB (65 nM) was added following a 100 s interval (to account for background fluorescence) and allowed to equilibrate for 200 s prior to the addition of $sPLA_2$ (70 nM final). Fluorescence intensities were monitored an additional 5 min. Hydrolysis was quantified by calculating the value of GP at 100 s after addition of enzyme and normalized for equivalence between microvesicle preparations (using protein content) and erythrocyte samples as described (Smith et al., 2001).

Two-Photon Microscopy

Scanning two-photon excitation microscopic images were collected on an Axiovert 35 inverted microscope (Zeiss, Thornwood, NY) at the Laboratory for Fluorescence Dynamics (Urbana, IL) as explained previously (Harris et al., 2001; Smith et al., 2001; Yu et al., 1996). The excitation source was a titanium-sapphire laser (Coherent, Palo Alto, CA) tuned to 780 nm and pumped by a frequency-doubled Nd:vanadate laser (Coherent).

For visualization of laurdan GP values, dual images were collected simultaneously using two detectors, a dichroic beamsplitter and emission interference filters (Ealing [now Optikos; Cambridge, MA] 440 and 490). Images of the GP values were calculated as described (Yu et al., 1996). In preparation for the images, washed erythrocytes (1.5% hct) were incubated for 1 h with 2.5 μM laurdan in MBSS (36°C). Cells were then washed and diluted to 2 ml in MBSS and allowed to settle in a temperature-controlled microscopy dish (Bioptechs, Butler, PA) for 15 min at 36–37°C. Following equilibration, multiple two-photon images were obtained before and after addition of ionomycin (300 nM) or control vehicle (DMSO).

Results

We used vesicles composed of DPPC with or without 30% cholesterol at various temperatures to set a standard for comparison among lipid phases that vary with respect to order and fluidity. Another probe that has been used frequently to study lipid phases in artificial and biological membranes, DPH, was included for comparison. Previous studies of the DPPC/cholesterol phase diagram revealed that laurdan emission spectra (quantified as GP) are sensitive mostly to lipid order while laurdan anisotropy

senses order and membrane fluidity since both impact the rotational diffusion of the probe (Harris et al., 2002). This phenomenon was reproducible, as demonstrated in Figure 1A and B. Compared to the solid ordered phase (below 41.5°C, pure DPPC), laurdan GP was slightly elevated in the liquid ordered phase (30% cholesterol). GP values range from 1 to −1. High values indicate a lack of interaction between laurdan and water molecules, typical of a membrane composed of ordered lipids. In contrast, low values are obtained as a consequence of the solvent relaxation phenomenon associated with laurdan-water interactions when membrane lipids are disordered as in the liquid disordered phase (above 41.5°C, pure DPPC in Fig. 1A) (Parasassi et al., 1991). In contrast to the results with laurdan GP, laurdan anisotropy decreased in the liquid ordered compared to the solid ordered phase. This result indicates that the probe is more mobile with respect to its ability to rotate when in the liquid ordered phase, presumably because of the increase in membrane fluidity. Both GP and anisotropy were higher in the liquid ordered than in the liquid disordered phase. In this case, even though both phases are considered "liquid" because of high translational lipid mobility, the tighter packing of lipids in the liquid ordered phase constrains the rotational mobility of the probe and therefore increases the anisotropy. The anisotropy of DPH behaved similarly to that of laurdan (Fig. 1C).

Figure 2A displays values of laurdan GP for samples of human erythrocytes before and after treatment with ionomycin, a calcium ionophore. Addition of ionomycin caused a large increase in the value of GP consistent with the membrane becoming more ordered, as reported previously (Best et al., 2002; Smith et al., 2001; Vest et al., 2004). As shown in Figure 2B, laurdan anisotropy (assessed simultaneously with GP) also rose upon ionomycin treatment. Parallel experiments using DPH as the probe appeared to give a similar result, although the increase in anisotropy was more subtle (Fig. 3).

Prior reports have suggested that the apparent increase in lipid order upon ionomycin treatment is not uniform spatially along the erythrocyte membrane (Best et al., 2002; Smith et al., 2001; Vest et al., 2004). Two-photon micrographs of human erythrocytes labeled with laurdan before (Fig. 4A) and after (Fig. 4B) ionomycin treatment confirmed this observation. These images show in false color the distribution of high (yellow/red) and low (blue/green) GP values along the surface of the cells. Figure 5 verifies that the elevated GP in ionomycin-treated cells was consistent among multiple images. The fact that the laser light used as an excitation source in two-photon experiments is naturally polarized allowed us to also explore whether the increase in average laurdan anisotropy upon ionomycin treatment observed in Figure 2B was uniform across the cell surface.

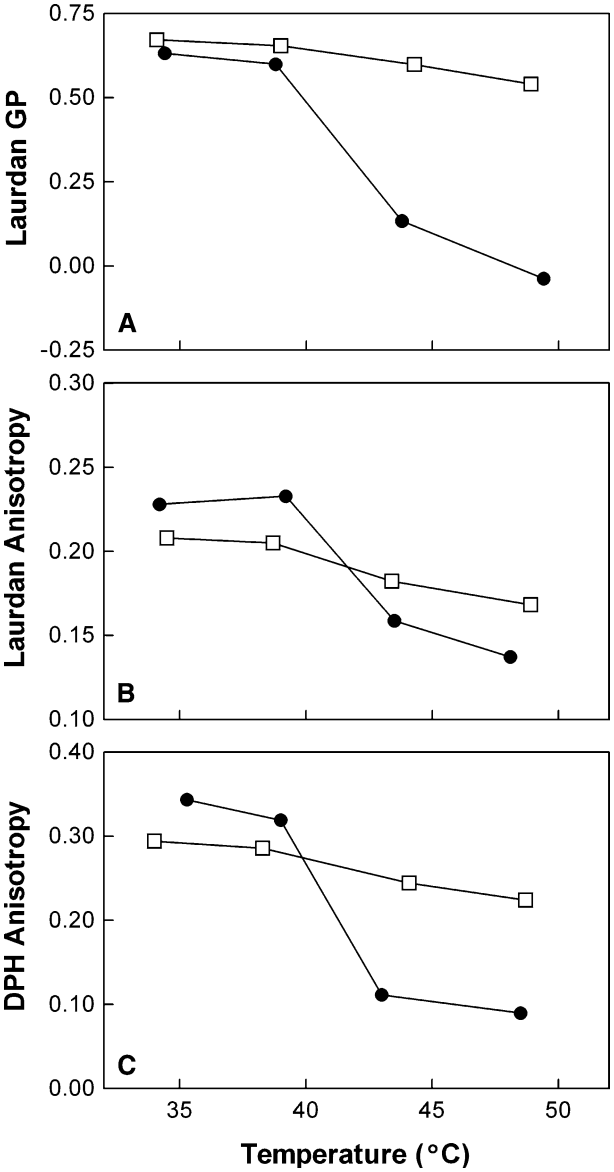

Fig. 1. Temperature dependence of laurdan emission spectra (*A*), laurdan anisotropy (*B*), and DPH anisotropy (*C*) in liposomes composed of pure DPPC (*solid circles*) or DPPC with 30% cholesterol (*open squares*). See Materials and Methods for experimental details.

As shown in Figure 4C, preferential excitation of laurdan in regions of the membrane parallel with the vector of polarization (arrow) occurs when the fluidity of the probe's environment is low (Parasassi et al., 1997). This phenomenon occurs because fluorophores perpendicular to the plane of polarization possess insufficient mobility to diffuse into a configuration that aligns their excited state dipole moment with that of the excitation photons. Detailed descriptions of the physics associated with this effect can be found in Bagatolli & Gratton (2000) and Parasassi et al. (1997). Figure 4D displays the distribution of laurdan intensity following ionomycin

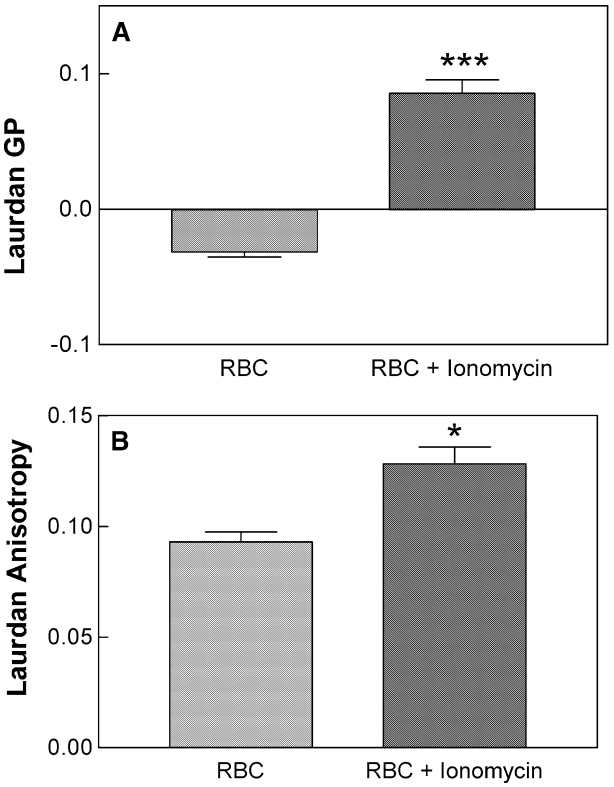

Fig. 2. Effects of ionomycin treatment on laurdan GP (*A*) and anisotropy (*B*) in human erythrocytes. Cells were incubated with laurdan, and emission spectra (quantified as GP) and steady-state anisotropy were successively measured before (*RBC*) and after ionomycin treatment on the same samples, as explained in Materials and Methods. All of the samples in *A* (n = 7–8) were assayed for both GP and anisotropy. The data in *A* were significant based on one-way analysis of variance (P = 0.0009 including data of Fig. 8A), and the group treated with ionomycin was significantly different from the control group (RBC) based on a posttest (Bonferroni, ***P < 0.001).The data in *B* were analyzed similarly in conjunction with Figure 8B (n = 10–16, P < 0.0001; *RBC* + *Ionomycin* compared to *RBC*, *P < 0.05).

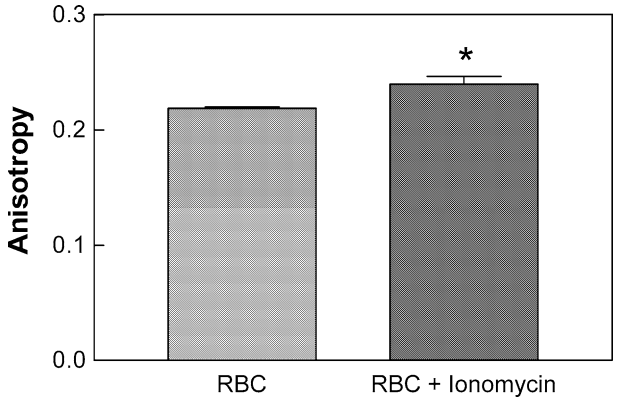

Fig. 3. Effects of ionomycin treatment on DPH anisotropy in human erythrocytes. Cells were incubated with DPH, and steady-state anisotropy was successively measured before (*RBC*) and after ionomycin treatment on the same samples, as explained in Materials and Methods. The data were significant based on one-way analysis of variance (P = 0.0006, n = 5, including the data of Fig. 9), and the group treated with ionomycin was significantly different from *RBC* based on a posttest (Bonferroni, *P < 0.05).

treatment. Although preferential excitation parallel to the polarization plane still occurred (indicating that fluorophore mobility was still at least somewhat restricted), a significant increase in the excitation of membrane regions perpendicular to the plane and an overall enhancement of fluorescence intensity was also observed. This result suggested that the environment of some of the laurdan molecules along the perimeter of the cells had actually become more fluid in the sense of allowing freer rotation of the probe (i.e., lower anisotropy), leading to more efficient excitation. Thus, even though the average anisotropy of laurdan in the cell membrane was higher after ionomycin treatment (Fig. 2B), this property, like the increase in average GP, was not uniform across the cell. Figure 6 illustrates a quantitative analysis of several images comparable to those of Figure 4 and demonstrates the reproducibility of the observation that the elevated GP along the cell perimeter after ionomycin treatment appeared to coexist with regions that displayed higher probe mobility.

The two-photon image in Figure 4B reveals small particles in the extracellular medium following ionomycin treatment. These particles presumably corresponded to the microvesicles known to be shed from human erythrocytes after ionophore treatment (Allan et al., 1980; Chukhlovin, 1996; Fourcade et al., 1995; Salzer et al., 2002; Smith et al., 2001). On the average, these microvesicles displayed a higher GP value than the cells from which they originated (Fig. 5). This tendency toward higher GP values was also reproducible when assessed among several microvesicle preparations in bulk suspension (Fig. 7A). Figure 7B and C demonstrates that these microvesicles also possessed other expected properties: enhanced exposure of PS on the outer leaflet of the membrane and elevated susceptibility to hydrolysis by $sPLA_2$ (Comfurius et al., 1990; Fourcade et al., 1995; Salzer et al., 2002).

To explore further the response of laurdan to these microvesicles, we continued the experiments of Figure 2 assessing both laurdan GP and steady-state anisotropy (Fig. 8; data of Fig. 2 included to facilitate comparison). After treatment of erythrocytes with ionomycin, samples were centrifuged to remove cells and the fluorescence in the microvesicles remaining in the supernatant was assayed. Figure 8A indicates that the level of laurdan GP observed in microvesicles was elevated relative to control erythrocytes and similar to that identified in ionophore-treated erythrocytes. However, the value of laurdan anisotropy was significantly reduced in the microvesicles compared to the membranes from which they originated. Figure 9 displays a similar result for samples containing DPH instead of laurdan.

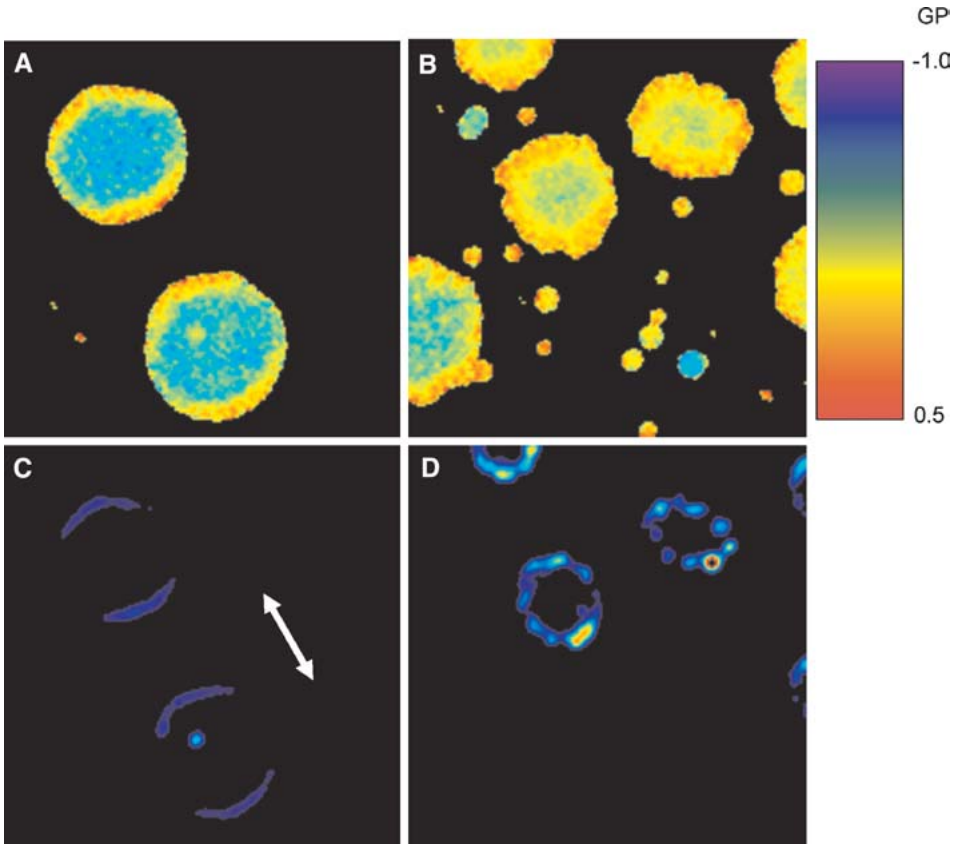

Fig. 4. Two-photon images of human erythrocytes before (*A, C*) and after (*B, D*) incubation with ionomycin. See Materials and Methods for experimental details. (*A, B*) False color represents laurdan GP values as indicated. (*C, D*) False color represents laurdan intensity. In these images, a minimum intensity threshold equal to twice the average original intensity was subtracted so that the effects of excitation polarization could be readily discerned (microvesicles and one of the cells from *B* are not visible in *D* because their fluorescence intensity was below the minimum). These images were collected using the 440 nm interference filter (see Materials and Methods; data with the 490 nm filter were comparable).

Recent evidence has suggested that the effect of intracellular calcium to increase erythrocyte membrane order may involve, at least in part, direct binding of calcium ions to the inner leaflet of the cell membrane (Vest et al., 2004). If the differences between microvesicles and erythrocytes observed in Figures 5, 7, and 8 reflect structural alterations to the membranes, they should not depend on calcium binding. We therefore tested this prediction by incubating the microvesicles with a calcium chelator, EDTA (20 mM). Since ionomycin would still be present in the microvesicle samples, EDTA added to the medium would remove both intravesicular as well as extravesicular calcium. As shown by the last bars in Figure 8, chelation of calcium did not reverse the results. Therefore, we concluded that the fluorescence observations reflected intrinsic membrane properties rather than membrane perturbation by calcium adsorption.

Discussion

The results obtained with the membranes of liposomes of defined composition demonstrate that laurdan anisotropy and GP may change in the same direction or different directions depending on the phases of the lipids being compared (Fig. 1). For example, they change in the same direction when comparing solid ordered to liquid disordered phases or when comparing liquid disordered to liquid ordered phases. Opposite changes are observed, however, if the comparison is between solid ordered and liquid ordered phases: GP increases by a small amount, suggesting slightly enhanced lipid order, and anisotropy decreases, implying some relaxation of constraints on probe rotational mobility because of greater membrane fluidity. Of course, applying this information directly to biological membranes would be naive since the compositional complexity of the latter precludes any simple description of bilayer properties in terms of physical states. Nevertheless, the results from the liposomes serve as a useful guide for interpretation by establishing that laurdan GP values are especially sensitive to lipid chain order while anisotropy (of either laurdan or DPH) provides additional information regarding fluidity. Thus, we draw the following conclusions based on the observations with erythrocytes and microvesicles and the standards in Figure 1:

1. Calcium loading of erythrocytes changes the membrane so that the average properties represent increased lipid order (i.e., increased laurdan GP in Figs. 2A, 4, and 5) and greater constraints on probe mobility (i.e., increased laurdan and DPH

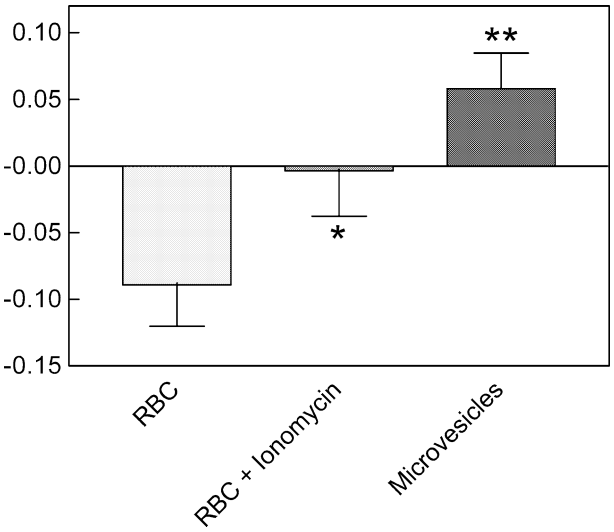

Fig. 5. Average laurdan GP values for erythrocytes and microvesicles from two-photon images. Multiple images were obtained as described in Figure 4. Average GP values were obtained from the images for cells prior to ionomycin treatment (*RBC*, total of 59 cells), after ionomycin treatment (*RBC + Ionomycin*, total of 110 cells), and for noncellular particles in ionomycin-treated samples (*Microvesicles*). These particles averaged 9.7% of image pixels. Fluorescent particles (presumably debris) in the absence of ionomycin treatment (as in Fig. 4A) were rare (0.98% of image pixels; $P = 0.007$ by two-tailed paired *t*-test compared to ionomycin-treated samples, $n = 5$ independent blood samples). GP values from the three groups were significant by analysis of variance ($P = 0.004$, $n = 5$ blood samples). Based on Bonferroni's post-test, RBC was significantly different from *RBC + Ionomycin* (*$P < 0.05$) and from *Microvesicles* (**$P < 0.01$).

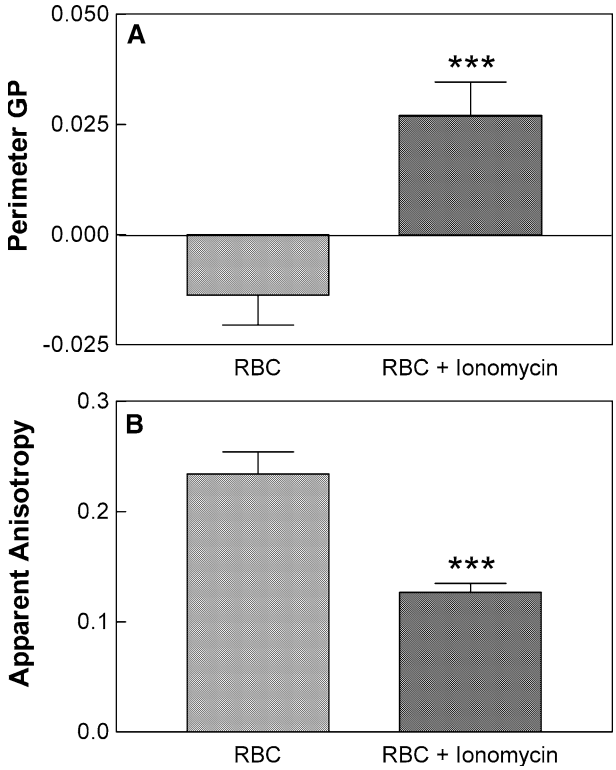

Fig. 6. Comparison of apparent laurdan anisotropy and GP along the perimeter of erythrocytes. Multiple images were obtained as described in Figure 4. (*A*) The total intensity of fluorescence observed through the 440 nm interference filter was sampled at the pole of the cells parallel to the excitation dipole (e.g., at the top of the cells in Fig. 4A) and from an equivalent area on the equator perpendicular to the excitation dipole (e.g., at the side edge of the cells in Fig. 4A). Apparent anisotropy values were then calculated from these intensities using equation 1 and assuming that G = 1. (*B*) GP values for each cell were sampled from the entire perimeter of the cells, sampling the same distance in from the edge as was done for *A* (27.6 ± 6.2% of the cell radius [mean ± SD], 47.2 ± 8.9% of the cell area). Data were collected from 16 images each for control (*RBC*, total of 46 cells) and ionomycin-treated (95–103 cells) samples. Differences between control and ionomycin-treated cells were significant (***$P \leq 0.001$ by unpaired two-tailed *t*-test in both cases).

anisotropy in Figs. 2B and 3). This result may be analogous to the situation observed in liposomes when converting from a prevalence of liquid disordered structures to increases in either solid ordered or liquid ordered domains.

2. These average changes in lipid order and probe mobility are not uniform across the membrane. Since there was evidence for local increases in probe rotational mobility in the same membrane regions that had become more ordered (Figs 4 and 6), we propose that ionophore treatment increases the presence of liquid ordered microdomains in the membrane. Thus, although the overall mobility of laurdan is diminished by ionophore treatment, local mobility may be increased. A possible alternative explanation for the lowered anisotropy shown in Figure 6 is the presence of surface irregularities which arise in erythrocytes upon calcium loading (Harris et al., 2001). The presence of these irregularities along the left and right sides of the cells in the image would allow some probe molecules that were previously oriented perpendicular to the excitation vector to now be parallel. Surely, this scenario explains some of the emergence of fluorescence along the sides of the cells in Figure 4D. However, the same phenomenon along the membrane regions parallel to the polarization vector (top and bottom of the cells in Fig. 4C and D) would result in a net decrease in fluorescence intensity in those regions because some of the laurdan molecules would now be oriented perpendicular. Since the intensity increased in all orientations along the cell membrane after ionophore treatment (Fig. 4D), it seems likely that the original conclusion that laurdan detected local domains of enhanced mobility is also valid.
3. Lipids in the membranes of microvesicles were more ordered than native erythrocytes and similar to those of ionophore-treated cells based on

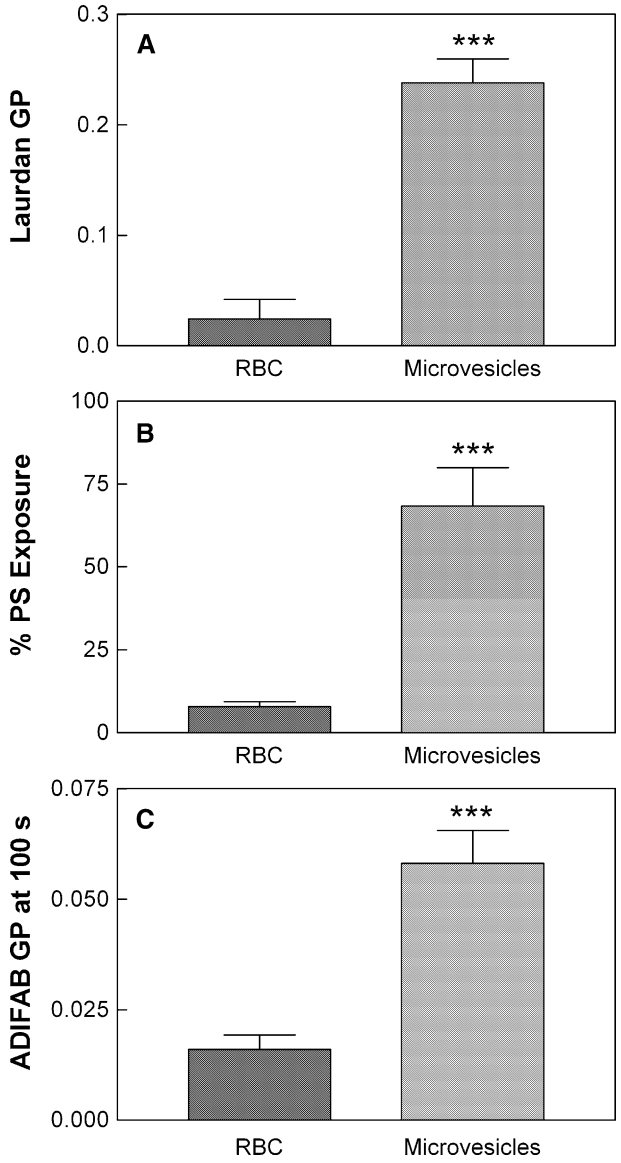

Fig. 7. Comparison of laurdan fluorescence (*A*), PS exposure on the outer membrane face (*B*), and susceptibility to PLA_2 (*C*) in untreated erythrocytes (*RBC*) and microvesicles. Microvesicles were prepared from calcium-loaded erythrocytes and laurdan fluorescence, PS exposure, and PLA_2 sensitivity were assayed as explained in Materials and Methods. In each panel, the difference is significant (***$P < 0.0001$) by unpaired two-tailed *t*-test (*A:* $n = 8$ RBC, $n = 13$ *Microvesicles*; *B:* $n = 10$ *RBC*, $n = 6$ *Microvesicles*; *C:* $n = 30$ *RBC*, $n = 13$ *Microvesicles*).

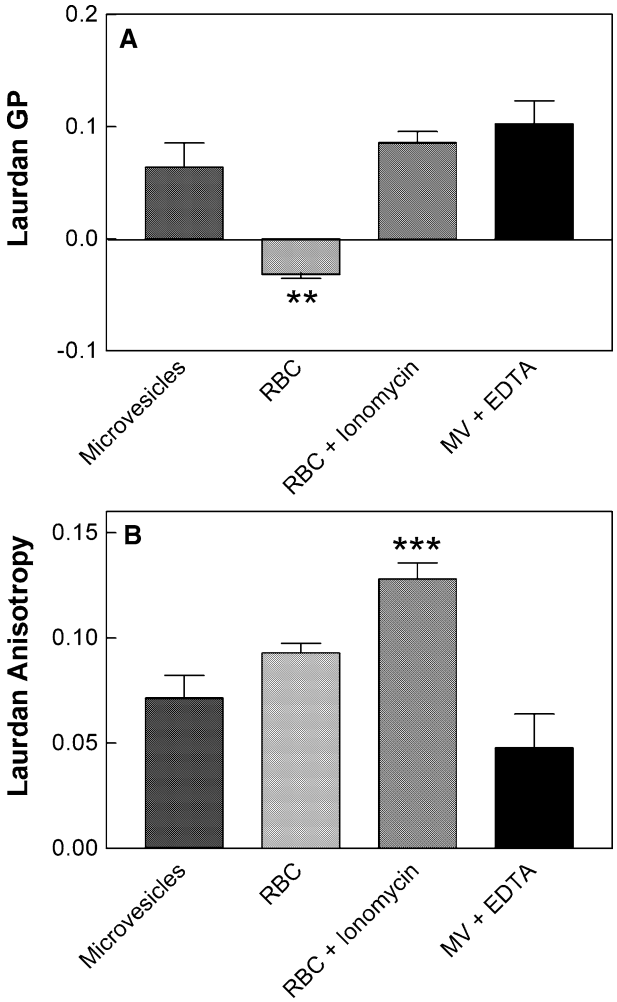

Fig. 8. Laurdan GP (*A*) and anisotropy (*B*) in microvesicles compared to erythrocytes with or without ionomycin and after EDTA treatment. Erythrocytes were incubated with laurdan, and emission spectra and steady-state anisotropy were successively measured before and after ionomycin treatment, following isolation of microvesicles, and after further incubation of microvesicles with EDTA (see Materials and Methods). The experiment is a continuation of that in Figure 2 (RBC and RBC + Ionomycin data are identical to Fig. 2), and the same samples were used for all experimental conditions ($n = 7$–8 in *A* and 10–16 in *B*). See Figure 2 for details of statistical analysis. Microvesicles were different from RBC (**$P < 0.01$) but indistinguishable from the other groups. The Microvesicles group in *B* was significantly different only from RBC + Ionomycin (***$P < 0.001$).

laurdan GP (Figs. 5, 7, and 8). Nevertheless, the average probe anisotropy was decreased compared to ionophore-treated cells. This result is reminiscent of that observed in liposomes when transferring from a membrane consisting largely of solid ordered domains to one composed of liquid ordered domains (Fig. 1) and is therefore consistent with the known liquid ordered propensity of microvesicle membranes (Gidwani et al., 2001). We believe that this result supports our proposal that combined use of laurdan steady-state emission and anisotropy can detect changes in liquid ordered structures in biological membranes. Nevertheless, it is critical to be absolutely clear that *order*, in this study, means the ability of solvent molecules (presumably water) in the immediate vicinity of laurdan to respond to the excited state dipole of the probe. *Fluidity* refers to the rotational mobility of the probe in the membrane.

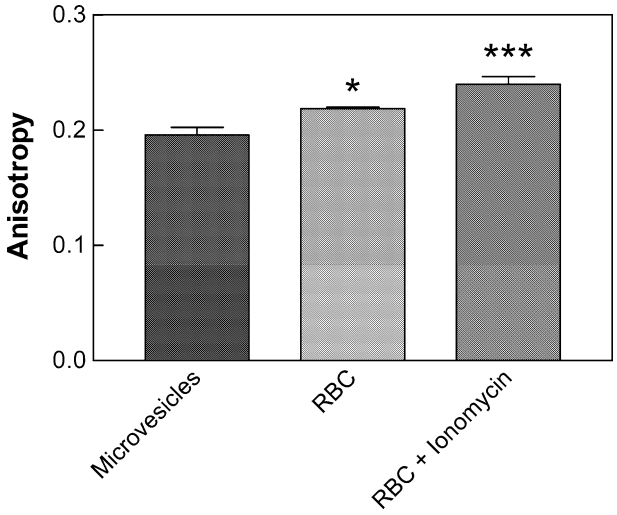

Fig. 9. DPH anisotropy in microvesicles compared to erythrocytes with or without ionomycin. Erythrocytes were incubated with DPH, and steady-state anisotropy was successively measured before and after ionomycin treatment and following isolation of microvesicles (see Materials and Methods). The experiment is a continuation of that in Figure 3, and the same samples were used for all experimental conditions. See Figure 3 for details of statistical analysis. The *Microvesicles* group in *B* was significantly different from both *RBC* (*$P < 0.05$) and *RBC + Ionomycin* (***$P < 0.001$).

> Thus, *liquid ordered* must be defined here as membrane domains with the property of limited solvent access or mobility concurrent with less constrained probe mobility.

A few issues regarding internal consistency of these results merit consideration. First, although microvesicles and ionomycin-treated cells consistently displayed elevated laurdan GP relative to untreated erythrocytes, the absolute values of these numbers varied among experiments (compare Figs. 2, 5, 7, and 8). This variation is partly due to the fact that these results were obtained from technical spectra acquired on different instruments with slightly different optical properties. The variation was more extreme with microvesicles (0.06 in Figs. 5 and 8 compared to 0.24 in Fig. 7) than with erythrocytes (-0.09 in Fig. 5 compared to 0.02 in Fig. 7). This discrepancy probably relates to relative levels of partitioning of laurdan into microvesicle membranes and the fact that higher concentrations of microvesicles were present in the experiments of Figure 7 (since they were added from concentrated samples prepared previously) than in Figures 5 and 8 (where microvesicles were in lower density because they were studied *in situ* as they were released from cells).

A second related issue concerns the numerical value of laurdan anisotropy in erythrocytes, which was low compared to that in liposomes (compare Figs. 1B and 2B). The reason for this difference is not known. Obviously, laurdan should be equally or more constrained in a cell membrane than in liposomes in the liquid disordered phase, as was observed for DPH (compare Figs. 3 and 1C). Artifacts due to sample light scatter or turbidity were excluded, as explained in Materials and Methods. It is possible that laurdan excited state lifetimes are longer in erythrocytes compared to vesicles, although since GP values were similar in erythrocytes to those in the liquid disordered phase of liposomes, this explanation seems unlikely. A more likely possibility is that laurdan partitioning is less in erythrocyte membranes than in liposome membranes, leading to a background component of probe anisotropy originating from laurdan micelles. This issue has been considered previously with respect to laurdan GP (Harris et al., 2001). The presence of hemoglobin complicates the issue and makes measurements of probe partitioning difficult. Nevertheless, we compensated for these challenges by repeating experiments with various methods that differ in their vulnerability to these artifacts (laurdan added directly to cell and microvesicle preparations in Fig. 7, repeated measures of the same samples following multiple treatments in Figs. 2 and 8, microscopy in Figs. 4–6, replication with DPH instead of laurdan). Therefore, the fact that trends in GP and anisotropy were consistent among these approaches lends credence to the basic conclusions notwithstanding the potential for artifacts.

This is not the first attempt to use environment-sensitive fluorescent probes to investigate liquid ordered domains in biological membranes. For example, the anisotropy of fluorescence-labeled phospholipids has been used to quantify the amount of order in the plasma membrane of cultured mast cells (Gidwani et al., 2001). In this case, it was assumed that the ordered lipids would represent the liquid ordered phase of membrane rafts. Likewise, the anisotropy of DPH has been used to provide comparative data regarding membrane fluidity and the prevalence of raft-like properties (Scheiffele et al., 1999). Two studies have made use of the steady-state fluorescence of laurdan to identify membrane regions of high lipid order. In one case, laurdan fluorescence was used to infer the presence of cholesterol-sensitive ordered domains in the lamellipodia of polarized neutrophils (Kindzelskii et al., 2004). Alternatively, two-photon microscopy was used to reveal large domains of high lipid order in macrophages. These domains colocalized with raft proteins such as caveolin and flotillin but excluded the transferrin receptor, a non-raft protein (Gaus et al., 2003).

The distinguishing feature of our approach is the dual use of fluorescence anisotropy and environment-sensitive emission spectra from a single probe. The other studies described above were significant in that they provided important, often quantitative,

information for biological membranes *in situ*. Nevertheless, conclusions were generally drawn based on the assumption that increased lipid order implies increased prevalence of rafts. The colocalization results provided compelling evidence for rafts in the macrophage studies (Gaus et al., 2003); however, these experiments involved the use of fixed cells, and it may be difficult to adapt them to conduct studies in real time during experimental manipulations of the cells. The combined use of laurdan anisotropy and GP has the advantage of exploiting the central distinguishing physical feature of liquid ordered phases – increased lipid order coupled with static or reduced membrane fluidity (Harris et al., 2002). Moreover, the additional information provided by two measurements may help refine interpretations made from a single parameter. For example, DPH is a common probe that has been used to assess both membrane "fluidity" and "order" from steady-state anisotropy measurements (Depauw et al., 1990; Gidwani et al., 2001; Jourd'heuil et al., 1996; Paila et al., 2005; Scheiffele et al., 1999). Based on the data of Figure 9, one would have concluded from DPH anisotropy that the membranes of microvesicles are less ordered than those of the cells from which they originated. The additional information provided by laurdan GP (Fig. 8) suggests a more detailed conclusion: that the membranes are similarly ordered but less constraining of the probe. Finally, the dual measurements with laurdan are beneficial in that they employ a single probe, can involve bulk samples or single cells, are quantitative, and can be performed *in vivo* in real time during experimental perturbation.

In addition to illustrating the ability of laurdan fluorescence to detect liquid ordered lipid behavior, the experiments in this report provided new information regarding the effect of ionomycin on the physical properties of erythrocyte membranes. This information is of interest because ionophore treatment of erythrocytes simulates changes that occur to cell membranes during cell injury and apoptosis (Chukhlovin, 1996), including enhanced susceptibility to digestion by $sPLA_2$ (Nielson et al., 2000; Smith et al., 2001). Previous work has suggested that erythrocyte membrane lipids become more ordered during ionophore treatment and that this ordering relates to the enhanced vulnerability to $sPLA_2$ (Best et al., 2002; Harris et al., 2001; Smith et al., 2001). Interestingly, increased hydrolysis occurs only under conditions at which the elevated lipid order occurs heterogeneously along the membrane surface, implying the importance of boundaries between domains of differential order (Best et al., 2002). The data of Figures 4 and 6 suggest that this ordering effect could actually represent propagation of liquid ordered membrane regions. Whether this alleged increase in liquid ordered properties is directly responsible for enhancing the ability of $sPLA_2$ to attack the membrane will require future investigations. Nevertheless, the observation that microvesicles, which do possess a high level of liquid ordered phase, also display high susceptibility to enzymatic action adds credence to this possibility.

This work was supported by grants from the National Science Foundation (MCB 9904597) and from the National Institutes of Health (GM073997). Fluorescence lifetime experiments were conducted at the Laboratory for Fluorescence Dynamics at the University of Illinois (Urbana, IL); gratitude is expressed to Drs. Theodore Hazlett and Enrico Gratton for providing technical assistance and access to the facility for these experiments. We also thank Mai Phong Vu for technical assistance with some of the experiments.

References

Allan, D., et al. 1980. The isolation and characterization of 60 nm vesicles ("nanovesicles") produced during ionophore A23187-induced budding of human erythrocytes. *Biochem. J.* **188:**881–887

Bacia, K., et al. 2004. Fluorescence correlation spectroscopy relates rafts in model and native membranes. *Biophys. J.* **87:**1034–1043

Bagatolli, L.A., Gratton, E.2000. Two photon fluorescence microscopy of coexisting lipid domains in giant unilamellar vesicles of binary phospholipid mixtures. *Biophys. J.* **78:**290–305

Barenholz, Y.2004. Sphingomyelin and cholesterol: from membrane biophysics and rafts to potential medical applications. *Subcell. Biochem.* **37:**167–215

Best, K., et al. 2002. Relationship between erythrocyte membrane phase properties and susceptibility to secretory phospholipase A_2. *Biochemistry* **41:**13982–13988

Bradford, M.M.1976. A rapid and sensitive method for the quantitation of microgram quantities of protein utilizing the principle of protein-dye binding. *Anal. Biochem.* **72:**248–254

Brown, D.2002. Structure and function of membrane rafts. *Int. J. Med. Microbiol.* **291:**433–437

Butikofer, P., et al. 1989. Enrichment of two glycosyl-phosphatidylinositol-anchored proteins, acetylcholinesterase and decay accelerating factor, in vesicles released from human red blood cells. *Blood* **74:**1481–1485

Chukhlovin, A.B.1996. Apoptosis and red blood cell echinocytosis: common features. *Scanning Microsc.* **10:**795–803

Comfurius, P., et al. 1990. Loss of membrane phospholipid asymmetry in platelets and red cells may be associated with calcium-induced shedding of plasma membrane and inhibition of aminophospholipid translocase. *Biochim. Biophys. Acta* **1026:**153–160

de Jong, K., Ott, P.1993. Membrane phospholipid asymmetry in DMPC-induced human red cell vesicles. *FEBS Lett.* **334:**183–188

Depauw, H., et al. 1990. Modification of the adenylate cyclase activity of bovine thyroid plasma membranes by manipulating the ganglioside composition with a nonspecific lipid transfer protein. *Biochim. Biophys. Acta* **1024:**41–48

Fourcade, O., et al. 1995. Secretory phospholipase A_2 generates the novel lipid mediator lysophosphatidic acid in membrane microvesicles shed from activated cells. *Cell* **80:**919–927

Gaus, K., et al. 2003. Visualizing lipid structure and raft domains in living cells with two-photon microscopy. *Proc. Natl. Acad. Sci. USA* **100:**15554–15559

Ge, M., et al. 1999. Electron spin resonance characterization of liquid ordered phase of detergent-resistant membranes from RBL-2H3 cells. *Biophys. J.* **77:**925–933

Gidwani, A., et al. 2001. Fluorescence anisotropy measurements of lipid order in plasma membranes and lipid rafts from RBL-2H3 mast cells. *Biochemistry* **40:**12422–12429

Harris, F.M., et al. 2001. Physical properties of erythrocyte ghosts that determine susceptibility to secretory phospholipase A_2. *J. Biol. Chem.* **276:**22722–22731

Harris, F.M., et al. 2002. Use of laurdan fluorescence intensity and polarization to distinguish between changes in membrane fluidity and phospholipid order. *Biochim. Biophys. Acta* **1565:**123–128

Jourd'heuil, D., et al. 1996. Membrane fluidity increases during apoptosis of sheep ileal Peyer's patch B cells. *Can. J. Physiol. Pharmacol.* **74:**706–711

Kindzelskii, A.L., et al. 2004. Cutting edge: optical microspectrophotometry supports the existence of gel phase lipid rafts at the lamellipodium of neutrophils: apparent role in calcium signaling. *J. Immunol.* **172:**4681–4685

Maraganore, J.M., et al. 1984. A new class of phospholipases A_2 with lysine in place of aspartate 49. Functional consequences for calcium and substrate binding. *J. Biol. Chem.* **259:**13839–13843

Nielson, K.H., et al. 2000. Susceptibility of S49 lymphoma cell membranes to hydrolysis by secretory phospholipase A_2 during early phase of apoptosis. *Biochim. Biophys. Acta* **1484:**163–174

Paila, Y.D., et al. 2005. The cholesterol-complexing agent digitonin modulates ligand binding of the bovine hippocampal serotonin 1A receptor. *Mol. Membr. Biol.* **22:**241–249

Parasassi, T., et al. 1991. Quantitation of lipid phases in phospholipid vesicles by the generalized polarization of laurdan fluorescence. *Biophys. J.* **60:**179–189

Parasassi, T., et al. 1997. Two-photon fluorescence microscopy of laurdan generalized polarization domains in model and natural membranes. *Biophys. J.* **72:**2413–2429

Richieri, G.V., Kleinfeld, A.M.1995. Continuous measurement of phospholipase A_2 activity using the fluorescent probe ADIFAB. *Anal. Biochem.* **229:**256–263

Salzer, U., et al. 2002. Ca^{++}-dependent vesicle release from erythrocytes involves stomatin-specific lipid rafts, synexin (annexin VII), and sorcin. *Blood* **99:**2569–2577

Scheiffele, P., et al. 1999. Influenza viruses select ordered lipid domains during budding from the plasma membrane. *J. Biol. Chem.* **274:**2038–2044

Simons, K., Ikonen, E.1997. Functional rafts in cell membranes. *Nature* **387:**569–572

Simons, K., Toomre, D.2000. Lipid rafts and signal transduction. *Nat. Rev. Mol. Cell Biol.* **1:**31–39

Smith, S.K., et al. 2001. Mechanisms by which intracellular calcium induces susceptibility to secretory phospholipase A_2 in human erythrocytes. *J. Biol. Chem.* **276:**22732–22741

Vest, R.S., et al. 2004. Divalent cations increase lipid order in erythrocytes and susceptibility to secretory phospholipase A_2. *Biophys. J.* **86:**2251–2260

Yu, W., et al. 1996. Fluorescence generalized polarization of cell membranes: a two-photon scanning microscopy approach. *Biophys. J.* **70:**626–636